

# Stringent Specificity in the Construction of a GABAergic Presynaptic Inhibitory Circuit

J. Nicholas Betley,<sup>1</sup> Christopher V.E. Wright,<sup>2</sup> Yoshiya Kawaguchi,<sup>3</sup> Ferenc Erdélyi,<sup>4</sup> Gábor Szabó,<sup>4</sup> Thomas M. Jessell,<sup>1,\*</sup> and Julia A. Kaltschmidt<sup>1,5</sup>

<sup>1</sup>Howard Hughes Medical Institute, Kavli Institute of Brain Science, Departments of Neuroscience, Biochemistry and Molecular Biophysics, Columbia University, New York, NY 10032, USA

<sup>2</sup>Program in Developmental Biology, Department of Cell and Developmental Biology, Vanderbilt University, Nashville, TN 37240, USA

<sup>3</sup>Department of Surgery and Surgical Basic Science, School of Medicine, Kyoto University, Kyoto, Japan

<sup>4</sup>Institute of Experimental Medicine, Department of Gene Technology and Developmental Neurobiology, Institute of Experimental Medicine, Budapest, Hungary

<sup>5</sup>Developmental Biology Program, Sloan-Kettering Institute, New York, NY 10003, USA

\*Correspondence: tmj1@columbia.edu

DOI 10.1016/j.cell.2009.08.027

## SUMMARY

GABAergic interneurons are key elements in neural coding, but the mechanisms that assemble inhibitory circuits remain unclear. In the spinal cord, the transfer of sensory signals to motor neurons is filtered by GABAergic interneurons that act presynaptically to inhibit sensory transmitter release and postsynaptically to inhibit motor neuron excitability. We show here that the connectivity and synaptic differentiation of GABAergic interneurons that mediate presynaptic inhibition is directed by their sensory targets. In the absence of sensory terminals these GABAergic neurons shun other available targets, fail to undergo presynaptic differentiation, and withdraw axons from the ventral spinal cord. A sensory-specific source of brain derived neurotrophic factor induces synaptic expression of the GABA synthetic enzyme GAD65 – a defining biochemical feature of this set of interneurons. The organization of a GABAergic circuit that mediates presynaptic inhibition in the mammalian CNS is therefore controlled by a stringent program of sensory recognition and signaling.

## INTRODUCTION

Neural coding in the mammalian central nervous system (CNS) relies on the ability of local inhibitory interneurons to filter information propagated by long-range excitatory pathways. Most inhibitory neurons release  $\gamma$ -aminobutyric acid (GABA), although this broad transmitter-based classification encompasses a diverse array of interneuron subtypes that display specialized synaptic features and form connections with distinct postsynaptic targets (Ascoli et al., 2008). The existence of many GABAergic interneuron subtypes greatly expands the repertoire of inhibitory coding strategies available to CNS circuits (Gupta

et al., 2000; Jonas et al., 2004). It also poses questions about the rules of specificity that govern the assembly of inhibitory circuits. Suggestions that GABAergic neurons seek out synaptic partners with high precision (Thomson and Morris, 2002; Stepanyants et al., 2004) have been countered by proposals that inhibitory networks can assemble in the absence of specificity cues (Li et al., 2007).

The plight of GABAergic interneurons reflects a more general uncertainty as to whether synaptic specificity in the mammalian CNS is based on stringent or hierarchical rules of target recognition. The prevailing view is that synaptic specificity is built not upon absolutes that restrict neurons to a single class of synaptic targets, but rather on a hierarchy of synaptic preferences (Sotelo, 1990; Shen, 2004). In this view, apparent instances of extreme specificity would belie a neuron's latent capacity to form connections with secondary targets. Genetic support for the hierarchical model has come primarily from studies in invertebrate nervous systems showing that removal of a preferred target invariably leads to the formation of ectopic synapses with new targets (Cash et al., 1992; Shen and Bargmann, 2003). In vertebrates, neurons grown in tissue culture typically form synapses with scant regard for target cell identity (Sanes and Poo, 1989). Nevertheless, in the intact mammalian CNS, it has not yet been possible to perform the invertebrate trick of eliminating a neuron's preferred target with precision and selectivity. As a consequence, there has been no decisive test of the dominance of stringent or hierarchical rules of recognition specificity during the construction of GABAergic, or indeed, any other mammalian CNS circuits.

Furthermore, synaptic specificity involves more than just target selection. Individual synapses need to be fine-tuned to the demands of the circuits in which they operate (Glickfeld and Scanziani, 2006). The diversity of GABAergic synapses is apparent in variant terminal morphologies, distinctions in the molecular machinery for exocytosis and, intriguingly, in the existence of dual pathways of GABA production (Kubota and Kawaguchi, 2000; Monyer and Markram, 2004). The synthesis of GABA is catalyzed by two distinct glutamic acid decarboxylase

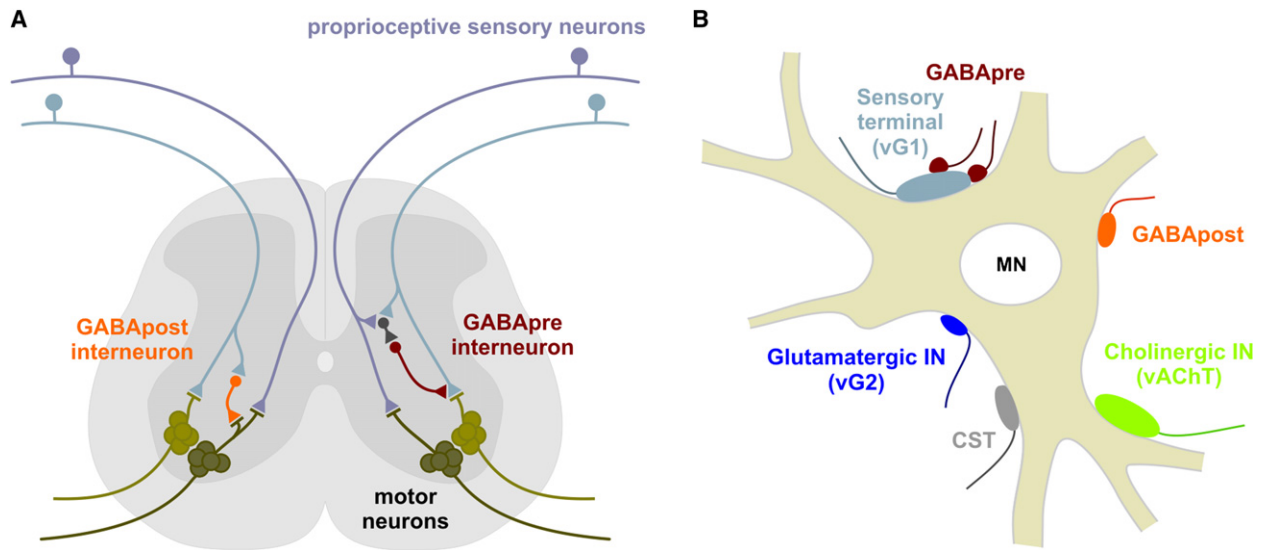


**Figure 1. Two GABAergic Inhibitory Circuits in the Spinal Cord**

(A) Circuitry of GABApre and GABApost neurons.

(B) Synaptic inputs on motor neurons include vGlut1 (vG1)<sup>+</sup> proprioceptive sensory terminals, GABApost terminals, vGlut2 (vG2)<sup>+</sup> interneuron terminals, vAChT<sup>+</sup> cholinergic interneuron terminals, and corticospinal terminals (CST). Proprioceptive terminals are contacted by GABApre terminals.

(GAD) enzymes. GAD67 is expressed in the cytosol of most GABAergic neurons, and is responsible for the bulk of neuronal GABA synthesis (Asada et al., 1997). In contrast, GAD65 is expressed by a more restricted set of interneurons (Escalpez et al., 1994), where it is bound to synaptic vesicles (Jin et al., 2003). The activity of GAD65 underlies enhanced GABA release at high stimulation frequencies (Tian et al., 1999), indicating that expression of this enzyme regulates the efficiency of inhibitory synaptic signaling. Defining rules of specificity that govern the construction of GABAergic synapses therefore also requires insight into mechanisms of presynaptic specialization and how they are coordinated with the events of target recognition.

The spinal circuits that control motor behavior have long provided a classical system for the exploration of inhibitory interneuron diversity and function. In the spinal cord, inhibitory interneurons assemble into feed-forward, feed-back, and reciprocal circuits that regulate sensory-motor reflexes (Jankowska and Puczyńska, 2008). Motor output is constrained by presynaptic inhibition of sensory transmitter release as well as by postsynaptic inhibition of motor neuron excitability (Figure 1A; Windhorst, 1996; Rudomin, 2009). The GABAergic synapses that participate in these two modes of inhibition are known to differ in their profile of GAD expression (Hughes et al., 2005), yet both synaptic classes coexist within the local micro-environment of the sensory-motor synapse (Figure 1B; Conradi, 1969). The distinct connectivity and synaptic features of these related classes of GABAergic interneurons suggested to us that they might provide an informative model system for probing two key issues in synapse assembly. Do neurons select their targets through stringent or hierarchical recognition systems? And what is the role, if any, of the target neuron in inducing the specialized presynaptic features that distinguish interneurons?

To explore these issues we used molecular genetics to manipulate identified neurons in mouse spinal cord. We find that the connectivity and synaptic features of GABAergic interneurons that mediate presynaptic inhibitory control of proprioceptive sensory input are directed by signals provided, selectively, by their sensory terminal targets. In the absence of target sensory terminals, this set of GABAergic neurons refuses to form connections with other available neurons, fails to undergo presynaptic differentiation, and eventually retracts their axons from the ventral spinal cord. We also show that brain derived neurotrophic factor (BDNF), a secreted factor emanating from proprioceptive sensory terminals, induces the synaptic localization of GAD65—a defining feature of these GABAergic interneurons. Thus, the sensory terminal targets of this specialized set of CNS inhibitory interneurons promote the development of their presynaptic partners through stringent, rather than hierarchical, programs of cell recognition.

## RESULTS

### GABAergic Synapses on Motor Neurons and Proprioceptive Sensory Terminals

We visualized the organization of monosynaptic sensory-motor reflex circuits in mouse spinal cord by monitoring expression of synaptic proteins from p6 to p40, over the period that these circuits mature. We identified motor neurons by green fluorescent protein (GFP) expression in *Hb9::GFP* transgenic mice (Figures 2A–2C). Proprioceptive sensory terminals on motor neurons were identified by coexpression of the vesicular glutamate transporter vGlut1 and Parvalbumin (Pv) (Figures 2D and 2E and Figures S1A–S1C available with this article online). These vGlut1<sup>+</sup> sensory terminals were distinguishable from vGlut2<sup>+</sup> interneuron inputs (Figure 2C), from vAChT<sup>+</sup> cholinergic interneuron terminals

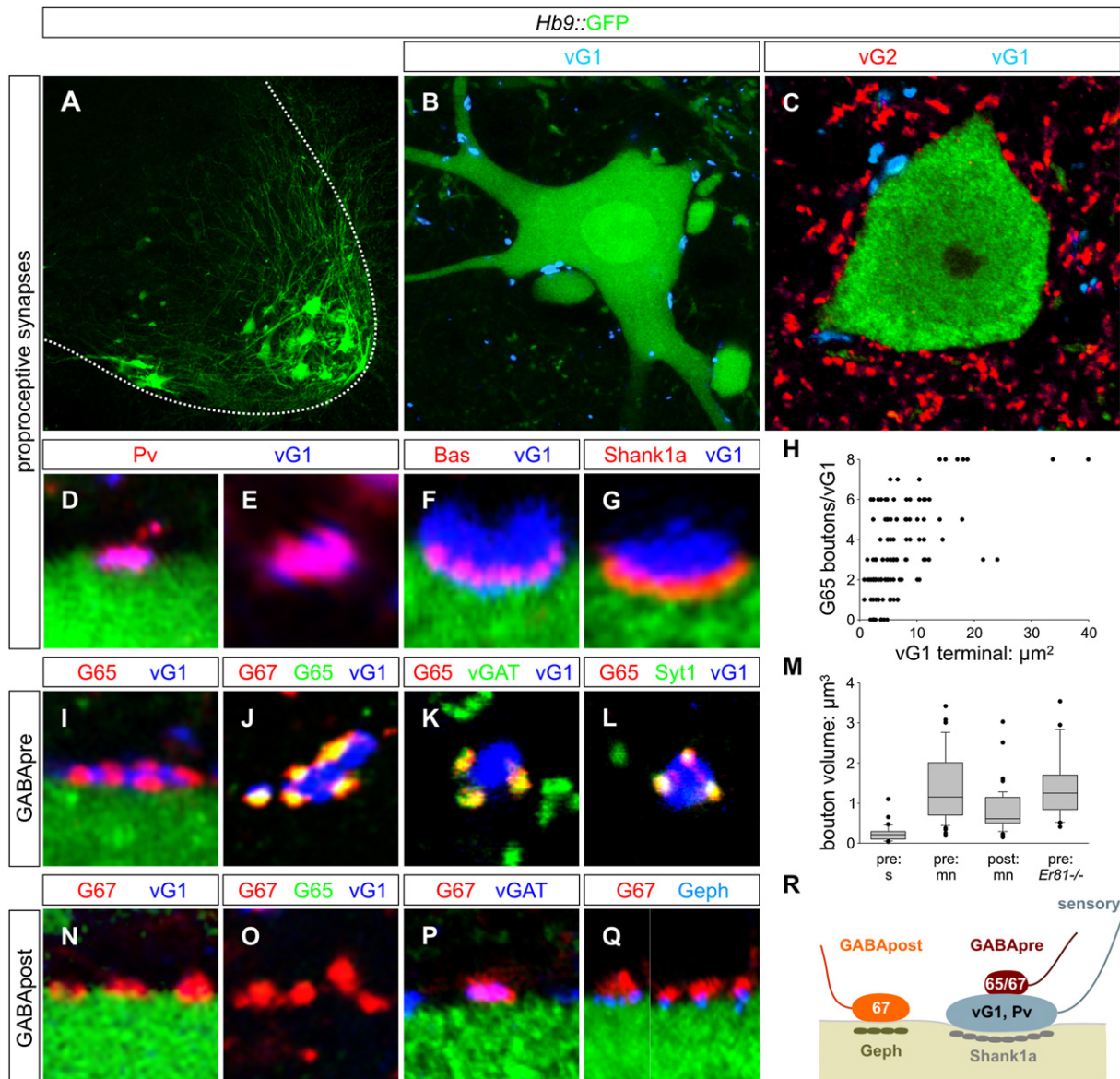


**Figure 2. Inhibitory Microcircuitry at Sensory-Motor Synapses**

(A) GFP<sup>+</sup> motor neurons.

(B and C) GFP<sup>+</sup> motor neurons contacted by vGlut1 (vG1)<sup>+</sup> and vGlut2 (vG2)<sup>+</sup> terminals.

(D and E) vG1<sup>+</sup> terminals on motor neurons coexpress Pv at p7.  $95.6 \pm 0.9\%$  vG1<sup>+</sup> terminals are labeled with mGFP in a *Pv::Cre*; *Tau:: $\phi$ mGFP* cross, indicating their sensory origin (Figure S1A–C) (for all quantitations herein, data are represented as mean  $\pm$  s.e.m.; n = 971 vG1<sup>+</sup> boutons; 3 mice).

(F) vG1<sup>+</sup> terminals express Bas at sites of contact with GFP<sup>+</sup> motor neurons.

(G)  $78.8 \pm 2.0\%$  of vG1<sup>+</sup> terminals (n = 259 boutons; 2 mice) on motor neurons align with postsynaptic Shank1a.

(H) GAD65 (G65)<sup>+</sup> boutons / vG1<sup>+</sup> terminal as a function of surface area of the vG1<sup>+</sup> terminal, at p15 to 21.  $89.9 \pm 3.1\%$  (n = 381 boutons; 2 mice) of vG1<sup>+</sup> terminals were contacted by at least one G65<sup>+</sup> bouton (n = 126 vG1<sup>+</sup> terminals, 3 mice).

(I–L) GAD expression by GABApre boutons.  $99.8 \pm 0.2\%$  (n = 746 boutons; 4 mice) of G65<sup>+</sup> terminals contact vG1<sup>+</sup> sensory terminals. > 99% of G65<sup>+</sup> boutons express GAD67 (G67), vGAT and Syt1.

(M) Distribution of the volumes of GABAergic boutons and varicosities in ventral spinal cord. Values obtained from > 100 bouton measurements in  $\geq 3$  mice. In each comparison, except between pre: mn contacts in the wild-type and *Er81<sup>-/-</sup>* background, differences are significant at  $p < 0.0001$  (Mann-Whitney U Test).

(N–Q) Synaptic marker expression at GABApost synapses. G67<sup>+</sup>, G65<sup>off</sup> terminals contact GFP<sup>+</sup> motor neurons, independent of proximity to vG1<sup>+</sup> sensory terminals. G67<sup>+</sup> terminals express vGAT.  $96.8 \pm 1.8\%$  (n = 339 boutons; 3 mice) of G67<sup>+</sup>, G65<sup>off</sup> terminals are aligned with motor neuron Geph<sup>+</sup> puncta.

(R) Inhibitory synaptic organization at sensory-motor synapses.

Images from rostral lumbar levels of p21 *Hb9::GFP* mice unless indicated.

(Figure S2A), and from corticospinal terminals (Figures S2I and S2J). We assigned synaptic status to vGluT1<sup>+</sup> sensory contacts with motor neurons on the basis of coexpression of Synapsin-1 (Syn1), SV2 and Bassoon (Bas), and alignment with the postsynaptic proteins Shank1a, PSD95 and GluR2/3 (Figures 2F, 2G, and S1D–S1G; Jin and Garner, 2008). Proprioceptive sensory terminals also contacted ventral interneuron populations, including Renshaw cells (Figures S2C–S2E; data not shown).

To define the organization of inhibitory inputs to this sensory-motor circuit, we monitored expression of GABA synthetic enzymes, the inhibitory amino acid transporters vGAT and GlyT2, GABA receptor subunits and the postsynaptic scaffolding protein Gephyrin (Geph). The composite expression profile of these proteins revealed two morphologically distinct classes of GABAergic boutons. One class is small (mean volume:  $0.24 \pm 0.04 \mu\text{m}^3$ ) and coexpresses GAD65, GAD67 and vGAT, but not GlyT2 (Figure 2I–K, S3C, D). The second class is larger ( $0.80 \pm 0.08 \mu\text{m}^3$ ), expresses GAD67 and vGAT, often GlyT2, but never GAD65 (Figure 2N–P, S3E, F). The small GAD65<sup>+</sup> boutons, but not the large GAD65<sup>off</sup> boutons, expressed the synaptic vesicle protein Synaptotagmin-1 (Syt1) (Figure 2L).

We found that these two classes of GABAergic boutons contribute to distinct microcircuits in ventral spinal cord, in general agreement with findings in rat (Hughes et al., 2005). In mice, > 99% of GAD65<sup>+</sup>, Syt1<sup>+</sup> boutons contacted proprioceptive sensory terminals, whether in association with motor neurons or interneurons (Figures 2L and S2F). Conversely, ~90% of sensory terminals on motor neurons were contacted by GAD65<sup>+</sup>, Syt1<sup>+</sup> boutons, with a mean innervation density of 3.2 GAD65<sup>+</sup>, Syt1<sup>+</sup> boutons per sensory terminal (Figure 2H). In contrast < 2% of the larger GAD65<sup>off</sup>, Syt1<sup>off</sup> boutons were juxtaposed to sensory terminals, and instead contacted cell bodies and dendrites of motor neurons (Figure 2N). We found that 97% of GAD67<sup>+</sup>, GAD65<sup>off</sup>, Syt1<sup>off</sup> boutons on motor neurons were aligned with postsynaptic  $\alpha 6$  and  $\beta 2/3$  GABA(A) receptor subunits, and Geph<sup>+</sup> puncta (Figures 2Q and S9). Viewed from the perspective of the sensory-motor synapse, we refer to the small, GAD65<sup>+</sup>, Syt1<sup>+</sup> sensophilic boutons as “GABApre” terminals, and the larger, GAD67<sup>+</sup>, GAD65<sup>off</sup>, Syt1<sup>off</sup> motophilic boutons as “GABApost” terminals (Figure 2R).

The restriction in expression of GAD65 and Syt1 to inhibitory boutons that contact sensory terminals permitted us to map the source of neurons that contribute to this specialized synaptic arrangement. From p15 onward, neurons expressing *Gad65*, *Gad67*, and *Syt1* were concentrated in the medial region of the deep dorsal horn and almost completely excluded from the ventral spinal cord (Figures S4A–S4E). These and other findings (Hughes et al., 2005) indicate that GABApre synapses derive from a small set of *Gad65*<sup>+</sup>, *Gad67*<sup>+</sup>, *Syt1*<sup>+</sup> neurons located in the medio-dorsal region of the spinal cord.

### Genetic Identification of GABApre and GABApost Interneurons

Can the interneurons that form GABApre and GABApost boutons be distinguished by molecular properties unrelated to their synaptic phenotype? We examined whether these two inhibitory interneuron classes, as with other spinal neurons (Stepien and Arber, 2008), express different transcription factors. *En1::Cre*

lineage tracing revealed that ~80% of GABApost boutons, but no GABApre boutons, derive from V1 interneurons (Figure S5). Since GABApre neurons are excluded from the ventral spinal cord, we turned to transcription factors that define neuronal subsets in the dorsal spinal cord. Expression of *Ptf1a* specifies a GABAergic interneuron class that settles in the dorsal spinal cord (Glasgow et al., 2005). We examined the connectivity of this set of interneurons by crossing a *Ptf1a::Cre* line with mouse reporter strains in which green or yellow fluorescent proteins (FP) are expressed upon excision of a floxed stop sequence.

In *Ptf1a::Cre*; FP reporter crosses, FP<sup>+</sup> neurons were detected in intermediate and dorsal domains of the spinal cord from e12.5 onward, but were excluded from the ventral domain (Figure 3A; Glasgow et al., 2005). At e16.5, FP<sup>+</sup> axons were detected in the ventral horn, but not near motor neurons (Figure S6A; data not shown). By p0 to p2, FP<sup>+</sup> axons contacted both sensory terminals and motor neurons (Figures S6B and S6C), but lacked detectable synaptic markers, notably GAD65 and GAD67 (Figures S6E–S6N). By p7, FP<sup>+</sup> contacts with sensory terminals expressed high levels of GAD65, GAD67, and other synaptic markers (Figures S6P and S6Q; data not shown), whereas contacts with motor neurons remained devoid of synaptic differentiation markers (Figures S6D, S6O, and S6R). By p15, as GABApre synaptic contacts attain maturity, 99% of compact FP<sup>+</sup> boutons contacting sensory terminals coexpressed GAD65, GAD67, Syt1 and other presynaptic markers (Figures 3B–3F). Conversely, 91% of GABApre boutons were FP-labeled in *Ptf1a::Cre*; *Tau:: $\Phi$ mGFP* mice. The few GABApre boutons that lacked FP expression appear to result from incomplete excision of the floxed stop sequence (Figure 3). FP<sup>+</sup> axons were still found in contact with motor neurons at p15, but their varicosities were large ( $1.46 \pm 0.15 \mu\text{m}^3$ ) and failed to concentrate GAD65, GAD67, Syt1 or other presynaptic markers (Figures 3G, 3I, S7A, and S7B). At these contact sites, the motor neuron membrane lacked expression of  $\alpha 6$  or  $\beta 2/3$  GABA receptor subunit proteins (Figures 3H and S9), although postsynaptic Geph<sup>+</sup> puncta were detected at ~50% of FP-labeled axonal contacts (Figures 3G, S7A–S7C, and S9). By p40, however, very few FP<sup>+</sup> boutons remained in contact with motor neurons (Figure S8), despite the persistence of sensory contacts. These findings establish that GABApre neurons form selective synaptic contacts with proprioceptive sensory terminals over the first postnatal week.

In addition, we asked if *Ptf1a*-marked GABAergic interneurons form presynaptic inhibitory contacts with the terminals of cutaneous sensory afferents located in the dorsal horn. *Ptf1a*-marked FP<sup>+</sup> boutons were observed in contacts with many cutaneous sensory terminals (Figures 3J–3M), revealing an intimate link between *Ptf1a* transcriptional provenance and the GABAergic interneurons responsible for presynaptic inhibition. Nevertheless, proprioceptive and cutaneous sensory terminals appear to be contacted by distinct subsets of *Ptf1a*-derived GABAergic interneurons (Figures 3J–3P; see Supplemental Data). Most FP<sup>+</sup> boutons on cutaneous sensory terminals expressed the glycine transporter GlyT2 and the neuropeptides enkephalin (ENK) and neuropeptide Y (NPY) (Figures 3K–3M), whereas these markers were not expressed by FP-labeled GABApre boutons in contact with proprioceptive sensory terminals (Figures 3N–3P). Thus, GABAergic interneurons destined to

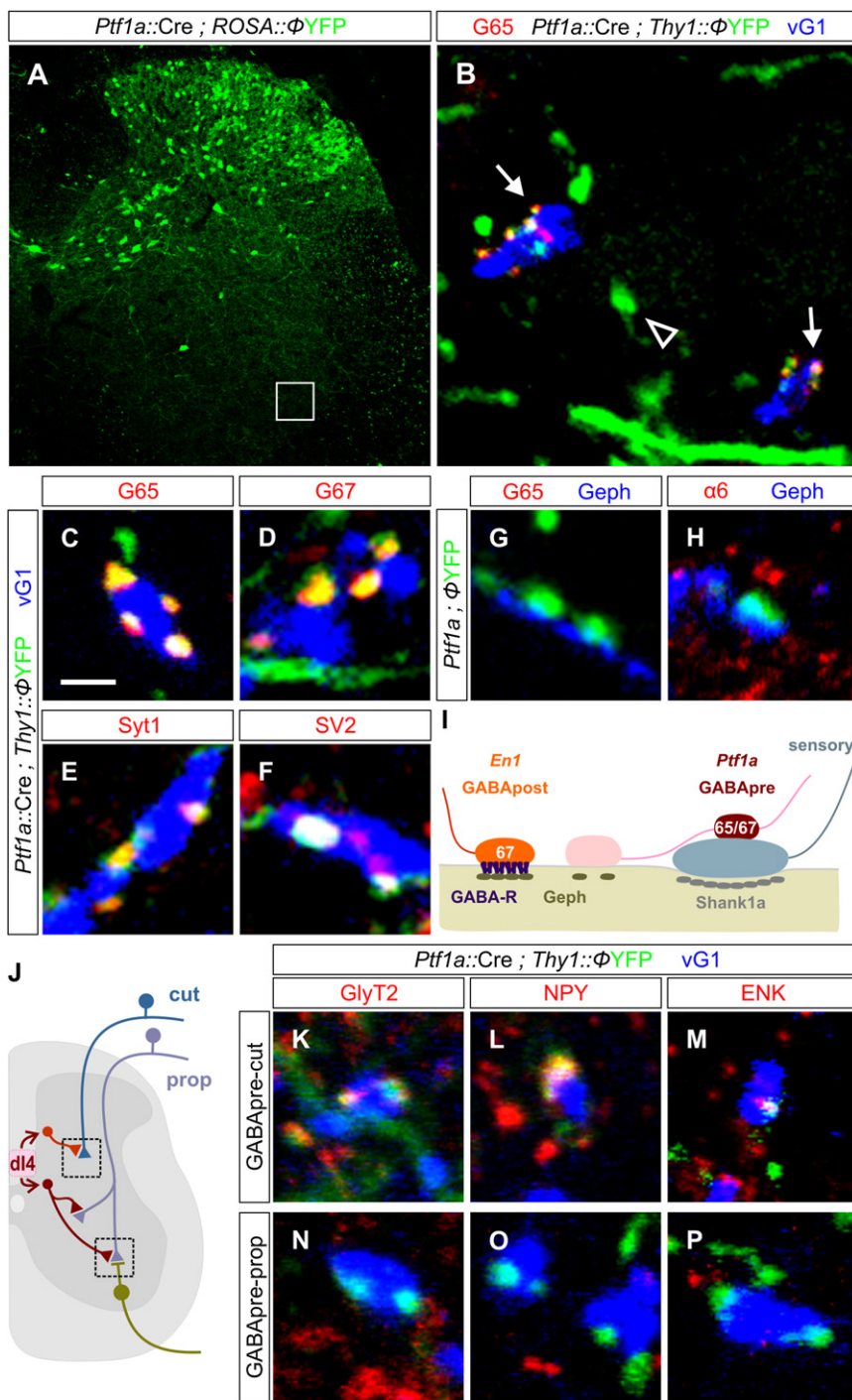


**Figure 3. Distinct Classes of *Ptf1a*-Derived GABApre Neurons Target Proprioceptive and Cutaneous Sensory Afferent Terminals**

(A) Dorsal restriction of YFP<sup>+</sup> neurons in *Ptf1a::Cre*; *ROSA::φYFP* mice.

(B) *Ptf1a::Cre*; *Thy1::φYFP* marked axons and terminals (subset of box in A). *Thy1::YFP*<sup>+</sup> axons (arrowheads) are observed in the vicinity of motor neurons. GAD65 (G65) expression is restricted to compact axonal boutons (arrows) on vGlut1 (vG1)<sup>+</sup> terminals.

(C–F) *Ptf1a::Cre*; *Thy1::φYFP*-labeled boutons on vG1<sup>+</sup> terminals express G65 (C), G67 (D), Syt1 (E), and SV2 (F). In *Ptf1a::Cre*; *Tau::φmGFP* mice, 90.9 ± 6.2% (n = 465 boutons; 3 mice) of G65<sup>+</sup> synapses on vG1<sup>+</sup> sensory terminals express mGFP. In many domains of the ventral horn ~100% of GABApre terminals express mGFP, suggesting G65<sup>+</sup>, mGFP<sup>off</sup> terminals result from inefficient Cre recombination.

(G and H) About 50% of *Ptf1a::Cre*; *Thy1::φYFP*-labeled GABApre axonal varicosities (see Figure 2M for volume) align with postsynaptic Geph<sup>+</sup> puncta but do not align with GABA<sub>A</sub> receptor α6 or β2/3 subunits (see Figure S9). These motor neuron-associated YFP<sup>+</sup> varicosities do not express G65 (G), G67, Syt1, Bas or SV2 (Figure S7A; data not shown).

(I) Neuronal target directs the differentiation of *Ptf1a*-marked GABApre boutons.

(J) *Ptf1a*-derived dI4 interneurons form synapses with cutaneous afferent terminals in the dorsal spinal cord and proprioceptive terminals in the ventral horn.

(K–M) In p15 *Ptf1a::Cre*; *Thy1::φYFP* mice, GABApre terminals synapse with vGlut1 (vG1)<sup>+</sup> cutaneous sensory terminals and express GlyT2 (K), NPY (L), and ENK (M).

(N–P) In p15 *Ptf1a::Cre*; *Thy1::φYFP* mice, GABApre terminals synapse with vG1<sup>+</sup> proprioceptive terminals, but do not express GlyT2 (N), NPY (O), or ENK (P).

Images from lumbar spinal cord of p21 mice. The scale bar represents 2 μm in (C)–(H) and (K)–(P).

target sensory terminals in the spinal cord are united by *Ptf1a* expression, but appear to diversify into distinct subsets based on the modality conveyed by their sensory target.

### Stringent Specificity of GABApre Connections with Proprioceptive Sensory Terminals

The observation that GABApre and GABApost neurons exhibit distinct transcriptional profiles before target contact argues

against the idea that they form synapses with sensory terminals or motor neurons in a random manner. The exclusive association of GABApre boutons with proprioceptive sensory terminals led us to examine the influence of the sensory target on the connectivity and differentiation of GABApre neurons.

To explore this issue we analyzed the differentiation of GABApre and GABApost synapses in mice lacking proprioceptive sensory terminals. We used two genetic strategies to eliminate proprioceptive sensory terminals from the ventral spinal cord. In mice mutant for the transcription factor *Er81*, sensory axons reach the intermediate region of the spinal cord, but very few of them project further ventrally (Figures 4A–4D; Arber et al., 2000). In *Pv::Cre*; *Isl2::φDta* mice, proprioceptive sensory

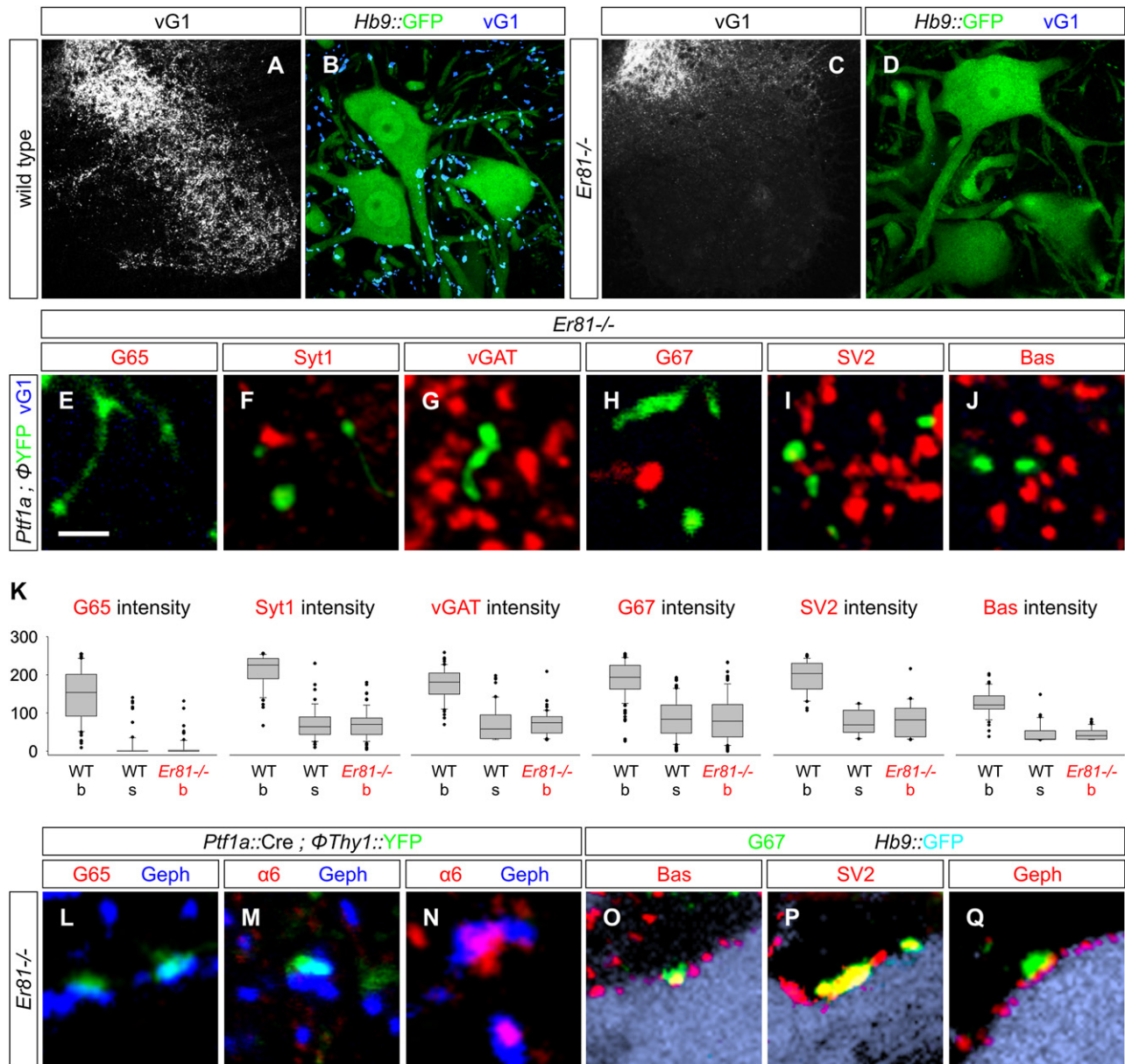


**Figure 4. GABApre Synaptic Differentiation Fails in the Absence of Sensory Terminals**  
 (A–D) vGlu1 expression in wild-type (A, B) and *Er81*<sup>-/-</sup> (C and D) spinal cord.  
 (E–J) Synaptic marker expression in YFP<sup>+</sup> GABApre axons and varicosities in the ventral horn of *Ptf1a::Cre; Thy1::φYFP; Er81*<sup>-/-</sup> mice.  
 (K) Synaptic protein levels in YFP<sup>+</sup> axon shafts (s) and boutons (b) in *Ptf1a::Cre; Thy1::φYFP* (wt) and *Ptf1a::Cre; Thy1::φYFP; Er81*<sup>-/-</sup> (*Er81*<sup>-/-</sup>) mice. Differences in protein level between wild-type and *Er81*<sup>-/-</sup> GABApre boutons/varicosities are significant at *p* < 0.0001 (Mann-Whitney U Test).  
 (L–N) In *Ptf1a::Cre; Thy1::φYFP; Er81*<sup>-/-</sup> mice, YFP<sup>+</sup> contacts on motor neurons are aligned with Geph<sup>+</sup> puncta, but are large and lack presynaptic G65 (L) and postsynaptic GABA<sub>A</sub> α6 (M). Geph<sup>+</sup> puncta lacking presynaptic YFP (GABApost) accumulate postsynaptic GABA<sub>A</sub> α6 (N).  
 (O–Q) In *Hb9::GFP; Er81*<sup>-/-</sup> mice, G67<sup>+</sup> terminals (green) contact GFP<sup>+</sup> motor neurons (light blue), coexpress Bas (O), SV2 (P) and vGAT (not shown), and align with motor neuron Geph<sup>+</sup> puncta (Q).  
 Images from p15 mice. The scale bar represents 2 μm in (E)–(J) and (L)–(Q).

neurons are killed by expression of diphtheria toxin (Dta), soon after their generation (Vrieseling and Arber, 2006). Analysis of *Er81*<sup>-/-</sup> and *Pv::Cre; Isl2::φDta* mice at p15 to p30 revealed a ~98% depletion of vGlu1<sup>+</sup> sensory terminals from the vicinity of motor neurons (Figures 4B, 4D, and S10A–S10C). The loss of

sensory afferent terminals did not alter the number of motor neurons, the patterning of their dendritic arbors, or the generation of ventral interneurons (data not shown; Vrieseling and Arber, 2006). These two strategies for sensory axon elimination elicited similar changes in the development and connectivity of

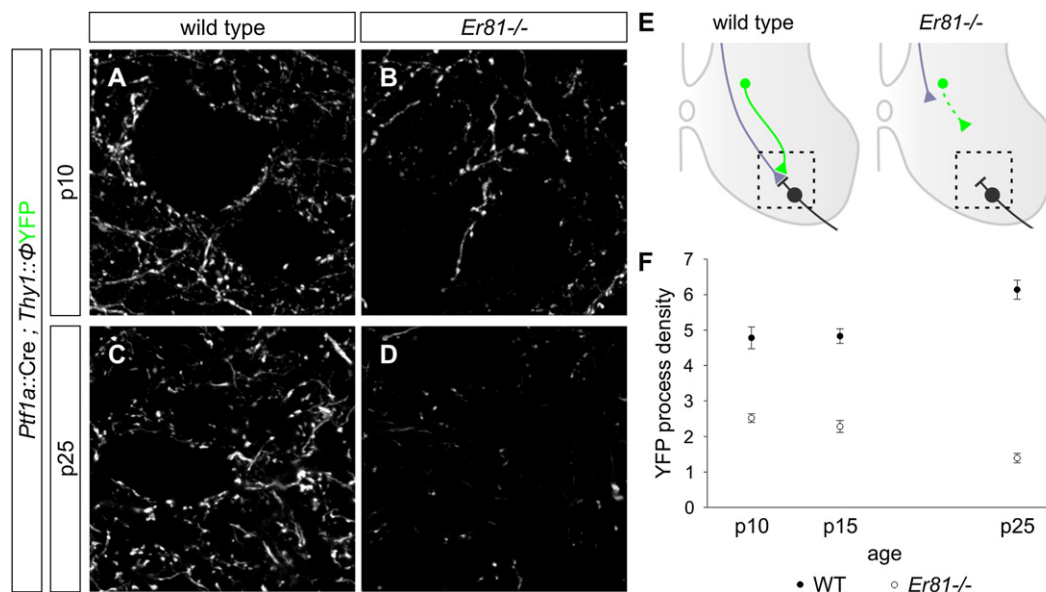


### Figure 5. Retraction of GABApre Axons in the Absence of Sensory Terminals

(A–D) YFP<sup>+</sup> axons in the ventral horn of *Ptf1a::Cre; Thy1::ΦYFP* (A, C) and *Ptf1a::Cre; Thy1::ΦYFP; Er81<sup>-/-</sup>* (B and D) mice. Images are 3 μm z-stacks from region marked in (E).

(E) Retraction of GABApre axons in *Er81<sup>-/-</sup>* mice (motor neurons in gray, sensory afferents in blue and GABApre axons in green).

(F) Density of YFP<sup>+</sup> axons and boutons in the ventral horn of *Ptf1a::Cre; Thy1::ΦYFP* (wt) and *Ptf1a::Cre; Thy1::ΦYFP; Er81<sup>-/-</sup>* (*Er81<sup>-/-</sup>*) mice at p10, p15 and p25. Error bars represent SEM. See Supplemental Experimental Procedures for quantitation.

GABApre neurons. We report detailed findings in *Er81* mutants, with a parallel analysis of *Pv::Cre; Isl2::ΦDta* mice presented in Supplemental Data (Figure S10).

We analyzed the connectivity and synaptic differentiation of GABApre axons in the absence of sensory terminals by crossing *Ptf1a::Cre* and FP reporter alleles into the *Er81* mutant background. At p10 to p15, many FP<sup>+</sup> axons and varicosities were detected in the ventral spinal cord despite the absence of sensory terminals (Figures 4E–4J). However, FP<sup>+</sup> GABApre axonal varicosities in *Er81* mutants had a mean volume ~6-fold greater than that of the GABApre boutons that contact sensory terminals in wild-type animals (Figure 2M). The FP<sup>+</sup> varicosities in *Er81* mutants also exhibited a 3- to 4-fold decrease in the concentration of GAD67 and other synaptic markers (Figures 4F–4K), presumably a reflection of protein dilution in these inflated axonal structures. In addition, we observed a ~17-fold decrease in the level of GAD65 expression, a reduction well beyond that of other synaptic markers (Figures 4E, 4K, and S11). Nevertheless, the terminals of the few proprioceptive axons that invade the ventral spinal cord in *Er81* mutants (Arber et al., 2000) were studied with fully differentiated GABApre boutons (Figure S12), precluding a sensory axon-independent influence of *Er81* on GABApre differentiation. Thus, the absence of sensory terminals results in a virtually complete loss of synaptic GAD65 and prevents GABApre boutons from acquiring their normal compact morphology.

We considered whether, in the absence of sensory terminals, GABApre neurons might switch target allegiance and attempt to form synapses with motor neurons. In *Er81* mutants examined at p15, we did detect FP<sup>+</sup> axonal varicosities in contact with motor

neurons, but these varicosities still lacked expression of GAD65, GAD67, vGAT and other presynaptic markers, and they were not aligned with postsynaptic α6 or β2/3 GABA(A) receptors (Figures 4L and 4M; data not shown). Thus GABApre boutons deprived of sensory terminals fail to acquire a GABApost-like connectivity pattern. Elimination of proprioceptive sensory terminals had no impact on the connectivity or differentiation of authentic GABApost boutons (Figures 4N–4Q). These findings indicate that the connectivity and synaptic differentiation of GABApre neurons exhibit an absolute dependence on sensory terminals. We also examined the fate of these synaptically unfulfilled GABApre axons by analyzing *Ptf1a::Cre*-induced FP reporter expression in *Er81* mutants at p25, the latest age that these mutants survive. We detected an ~80% reduction in the total number of FP-labeled axons and varicosities in the ventral spinal cord, compared to controls (Figures 5A–5F). Nevertheless, the number of *Gad65*<sup>+</sup>, *Ptf1a*-marked interneurons in the medio-dorsal domain of *Er81* mutants was similar to that in wild-type animals (Figure S13), providing evidence that GABApre neurons survive the loss of their sensory target, at least at this stage.

Thus, GABApre neurons deprived of their sensory targets do not form ectopic synapses with spinal neurons, and instead they undergo a complete failure of presynaptic differentiation and eventually withdraw their axons from the ventral spinal cord. These findings reveal that proprioceptive sensory terminals are the sole source of signals that direct the synaptic organization of GABApre neurons, arguing for unprecedented stringency in neuronal target recognition. They also raise the question of the molecular nature of these sensory-specific connectivity and presynaptic differentiation signals. We have

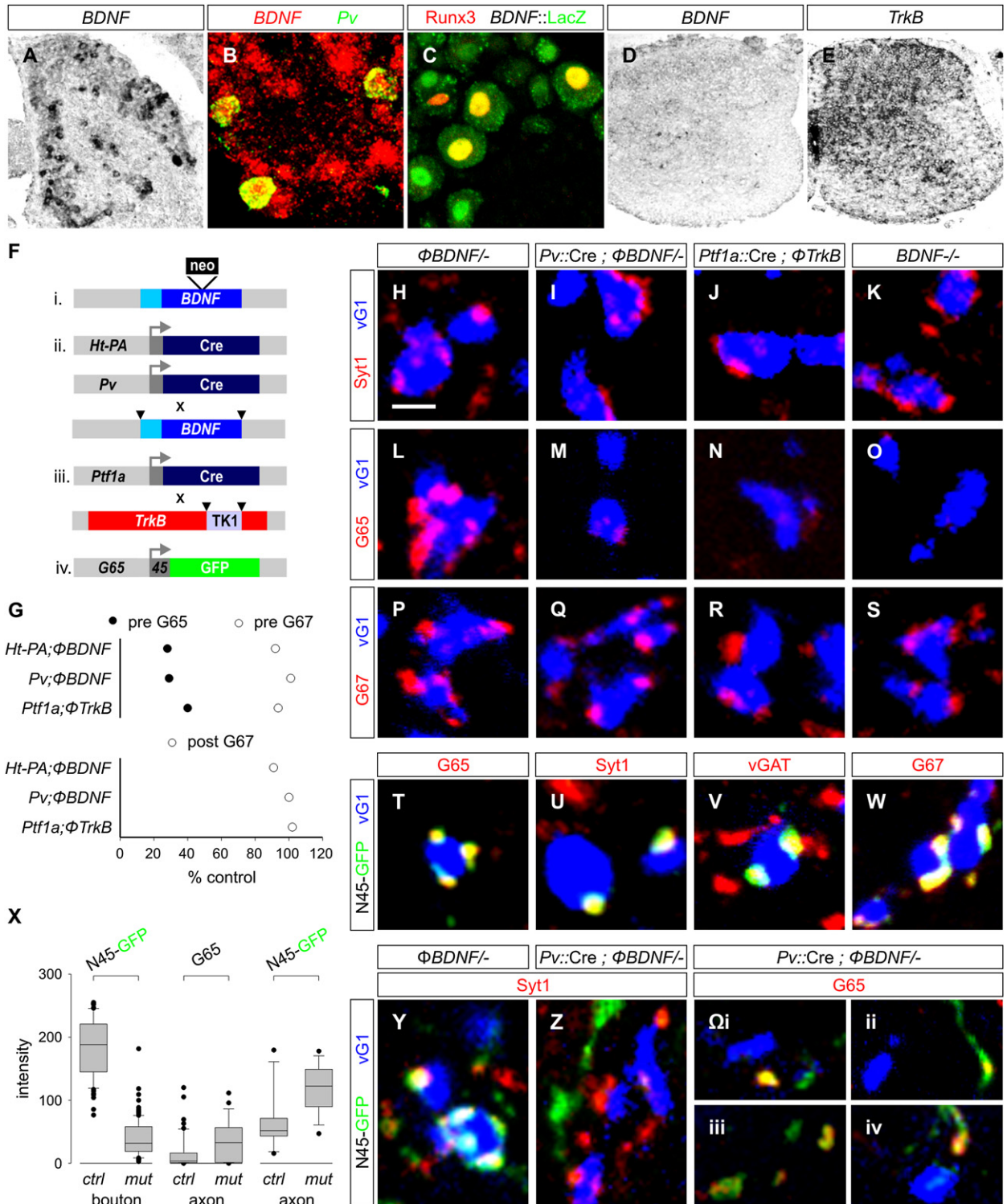


**Figure 6. Accumulation of GAD65 in GABApre Boutons Depends on Sensory-Derived BDNF Signaling**  
 (A)  $30.5 \pm 0.7\%$  ( $n = 464$  neurons; 3 mice) of p7 lumbar DRG neurons express *BDNF* mRNA.  
 (B)  $\sim 85\%$  ( $n = 3$  mice) of p7 *Pv*<sup>+</sup> proprioceptive neurons express *BDNF* mRNA.  
 (C)  $81.5 \pm 3.8\%$  ( $n = 54$  neurons; 2 mice) of *Runx3*<sup>+</sup> proprioceptive DRG neurons express LacZ in *BDNF::LacZ* reporter mice.  
 (D) *BDNF* expression in p7 spinal cord.  
 (E) *TrkB* expression in p7 spinal cord.



not defined the molecular basis of GABApreproprioceptive sensory terminal recognition, but have identified BDNF as the critical sensory terminal factor that directs the presynaptic differentiation of GABApre neurons, as described below.

### Sensory-Derived BDNF Directs Synaptic Accumulation of GAD65 in GABApre Neurons

The inability of motor neurons or interneurons to compensate for the loss of sensory terminals implies that spinal neurons lack relevant GABApre synaptic organizing signals. We therefore asked whether any of the known genes implicated in synaptic differentiation in the CNS (Huang and Scheiffele, 2008) exhibit sensory-specific profiles of expression. Of over fifty genes examined (Table S1) only *BDNF* exhibited a sensory-specific expression profile. In the first two postnatal weeks, the peak period of GABApre synaptic assembly, we found that *BDNF* mRNA (as well as LacZ in a *BDNF::LacZ* knock-in line) was expressed at a high level by ~30% of all DRG neurons, and in ~85% of proprioceptive sensory neurons, defined by *Pv* and *Runx3* expression (Figures 6A–6C). In contrast, *BDNF* expression was restricted to a few scattered spinal cord cells (Figure 6D). The high affinity BDNF receptor *TrkB* was expressed by many spinal cord neurons, including those in the medio-dorsal domain that constitutes the source of GABApre neurons (Figure 6E; data not shown).

To test whether BDNF-TrkB signaling controls the synaptic differentiation of GABApre neurons we used mouse genetics to eliminate BDNF selectively from proprioceptive sensory neurons and *TrkB* selectively from GABApre neurons (see Figure 6F for Cre driver strains and *BDNF* and *TrkB* mutant alleles). The loss of BDNF-TrkB signaling did not influence the differentiation of proprioceptive sensory terminals in the ventral spinal cord (Figure S14). Moreover, the number of *Gad65*<sup>+</sup> neurons in the medio-dorsal domain of the spinal cord was similar in wild-type, conditional *BDNF*, and conditional *TrkB* mutants (Figure S15; data not shown). Thus BDNF-TrkB signaling is not required for the survival of GABApre neurons, or for expression of the *Gad65* gene.

We next examined the synaptic phenotype of *BDNF* and *TrkB* mutant mice. The loss of BDNF-TrkB signaling did not prevent GABApre neurons from forming synapses, as revealed by the

persistence of Syt1<sup>+</sup> boutons on proprioceptive sensory terminals, even when assayed in adult animals (Figures 6H–6K and S16). Nevertheless, it did result in a dramatic reduction in the level of GAD65 in GABApre boutons (74%–85%, depending on the particular *BDNF* or *TrkB* mutants analyzed) (Figures 6G and 6L–6O). The influence of BDNF signaling was selective for this one feature of GABAergic synaptic differentiation. GABApre boutons expressed wild-type levels of GAD67 and other synaptic markers in all *BDNF* and *TrkB* mutant strains examined (Figures 6G, 6H–6K, and 6P–6S; data not shown). Moreover, the number and synaptic status of GABApost boutons was unaffected by the loss of BDNF-TrkB signaling (Figure 6G; data not shown). These findings provide evidence that the secretion of BDNF from proprioceptive sensory terminals activates *TrkB* receptors on GABApre neurons to promote the synaptic accumulation of GAD65.

Since *Gad65* gene expression in GABApre neurons is maintained in *BDNF* mutants, we asked whether the depletion of synaptic GAD65 results from a complete loss, or a redistribution, of the protein. The depletion of GAD65 from GABApre boutons was accompanied by a 4-fold increase in the level of protein expression in preterminal axons (Figure 6X,  $\Omega$ i-iv). To probe the basis of this redistribution, we analyzed a *Gad65::N<sup>45</sup>GFP* transgenic mouse line in which the N-terminal 45aa axonal trafficking domain of GAD65 (Kanaani et al., 2002) is expressed as a GFP fusion protein (<sup>N45</sup>GFP). In this line, the pattern of <sup>N45</sup>GFP<sup>+</sup> neurons in p7 to p30 spinal cord resembled that of the endogenous *Gad65* transcript: <sup>N45</sup>GFP<sup>+</sup> neurons were excluded from the ventral spinal cord and concentrated in the medio-dorsal domain, where ~40% of them (the presumed GABApre neurons) coexpressed a *Ptf1a::Cre* driven reporter protein (Figure S17).

We found that the 45aa trafficking domain of GAD65 is sufficient to direct synaptic accumulation of GFP in GABApre neurons. Over 95% of GABApre boutons in the ventral spinal cord of *Gad65::N<sup>45</sup>GFP* mice expressed <sup>N45</sup>GFP, and conversely > 99% of <sup>N45</sup>GFP<sup>+</sup>, Syt1<sup>+</sup> varicosities were associated with sensory terminals (Figures 6T–6W). We therefore crossed the *Gad65::N<sup>45</sup>GFP* allele into mice lacking proprioceptor BDNF and assayed the localization of <sup>N45</sup>GFP in GABApre neurons. At p21 we detected an ~5-fold decrease in the level of <sup>N45</sup>GFP in GABApre boutons and an associated ~4-fold

(F) Cre driver lines, *BDNF*, and *TrkB* alleles used.

(G) Relative levels of GAD65 (G65, filled circles) and GAD67 (G67, open circles) in GABApre terminals (top plot), and of G67 (open circles) in GABApost terminals (bottom plot) in mutant mice with impaired BDNF-TrkB signaling (1. *Ht-PA::Cre*;  $\phi$ *BDNF*<sup>-/-</sup> versus  $\phi$ *BDNF*<sup>-/-</sup> 2. *Pv::Cre*;  $\phi$ *BDNF*<sup>-/-</sup> versus  $\phi$ *BDNF*<sup>-/-</sup> 3. *Ptf1a::Cre*;  $\phi$ *TrkB* /  $\phi$ *TrkB* versus  $\phi$ *TrkB* /  $\phi$ *TrkB*). Differences between mutant and control genotypes are significant at  $p < 0.0001$  (Mann-Whitney U Test).

(H–K) Syt1<sup>+</sup> GABApre boutons contact vGlut1 (vG1)<sup>+</sup> terminals in (H)  $\phi$ *BDNF*<sup>-/-</sup> control, (I) *Pv::Cre*;  $\phi$ *BDNF*<sup>-/-</sup>, (J) *Ptf1a::Cre*;  $\phi$ *TrkB* /  $\phi$ *TrkB* and (K) *BDNF*<sup>-/-</sup> mice. (L–O) G65 expression in GABApre boutons on vG1<sup>+</sup> terminals in (L)  $\phi$ *BDNF*<sup>-/-</sup> control, (M) *Pv::Cre*;  $\phi$ *BDNF*<sup>-/-</sup>, (N) *Ptf1a::Cre*;  $\phi$ *TrkB* /  $\phi$ *TrkB* and (O) *BDNF*<sup>-/-</sup> mutant mice.

(P–S) G67 expression in GABApre boutons on vG1<sup>+</sup> terminals in (P)  $\phi$ *BDNF*<sup>-/-</sup> control, (Q) *Pv::Cre*;  $\phi$ *BDNF*<sup>-/-</sup>, (R) *Ptf1a::Cre*;  $\phi$ *TrkB* /  $\phi$ *TrkB* and (S) *BDNF*<sup>-/-</sup> mutant mice.

(T–W) In *Gad65::N<sup>45</sup>GFP* mice, <sup>N45</sup>GFP<sup>+</sup> boutons that contact vG1<sup>+</sup> terminals express G65 (T), Syt1 (U), vGAT (V), and G67 (W). In *Gad65::N<sup>45</sup>GFP* mice, 94.6 ± 1.8% (n = 205 boutons; > 5 mice) of G65<sup>+</sup> terminals express <sup>N45</sup>GFP.

(X) <sup>N45</sup>GFP expression intensity in GABApre boutons and axons in *Gad65::N<sup>45</sup>GFP*;  $\phi$ *BDNF*<sup>-/-</sup> (ctrl) and *Pv::Cre*;  $\phi$ *BDNF*<sup>-/-</sup> (mut) mice (see first and third columns, marked <sup>N45</sup>GFP) and endogenous G65 in axons (see middle column marked G65).

(Y) <sup>N45</sup>GFP expression in Syt1<sup>+</sup> GABApre boutons contacting vG1<sup>+</sup> terminals in  $\phi$ *BDNF*<sup>-/-</sup> mice.

(Z) <sup>N45</sup>GFP excluded from Syt1<sup>+</sup> GABApre boutons in *Pv::Cre*;  $\phi$ *BDNF*<sup>-/-</sup> mutant mice, but detected in axons near vG1<sup>+</sup> terminals.

( $\Omega$ i-iv) *Pv::Cre*;  $\phi$ *BDNF*<sup>-/-</sup> mutant spinal cords showing <sup>N45</sup>GFP and endogenous G65 accumulating at axons not in contact with vG1<sup>+</sup> terminals.

Images from p21 lumbar spinal cord unless indicated. The scale bar represents 2  $\mu$ m.

increase in the level of <sup>N45</sup>GFP in the preterminal axon (Figure 6Y-Ωiv), indicating that BDNF signaling regulates the synaptic accumulation of GAD65 through its N-terminal trafficking domain. Thus, a defining feature of GABApre synaptic differentiation—the accumulation of GAD65 in synaptic terminals—is controlled by the release of BDNF from proprioceptive sensory terminals.

## DISCUSSION

Inhibitory circuits in the mammalian CNS are organized with remarkable precision. Our analysis of a GABAergic presynaptic inhibitory circuit involved in the gating of spinal sensory-motor transmission reveals that its assembly is directed by an unusually stringent program of wiring specificity that has its origins in the selectivity of expression of recognition and synaptic differentiation signals by proprioceptive sensory terminals.

### Stringent Specificity in the Assembly of an Inhibitory Synapse

In the ventral spinal cord, proprioceptive sensory terminals are the sole synaptic target of GABApre neurons, yet they scrupulously avoid input from GABApost neurons. We estimate that GABApre neurons exhibit a sensory:motor preference of nearly 2000:1 (see Supplemental Experimental Procedures). The fact that GABApre and GABApost neurons are distinguishable by transcriptional profile prior to, and independent of, target contact, excludes the possibility that the striking specificity of this presynaptic inhibitory circuit emerges in a haphazard manner (see Supplemental Discussion).

Our findings provide insight into the strategies used to achieve synaptic specificity in CNS circuits, and whether connections form through absolute or hierarchical programs of target recognition. In invertebrate circuits, analysis of synaptic specificity has provided persuasive evidence for the operation of hierarchical recognition systems (Shen, 2004). In *C. elegans*, removal of the epithelial cells that determine the synaptic target profile of motor neurons leads to a shift in synaptic partner, to a distinct group of muscle cells (Shen and Bargmann, 2003; Shen et al., 2004). Similarly, elimination of the normal target muscle of *Drosophila* motor neurons leads to the ectopic innervation of substitute muscles (Cash et al., 1992). Transposed to the spinal cord, this hierarchical view of synaptic specificity predicts that proprioceptive sensory terminals represent only a preferred target for GABApre neurons, with motor neurons and ventral interneurons able to serve as alternative synaptic partners under conditions of sensory terminal deprivation. Our findings argue against this hierarchical scheme, at least in the context of presynaptic inhibitory synapses. We find that GABApre axons deprived of their proprioceptive sensory terminal targets fail to form synapses with other nearby neurons. Moreover, the rejection of all synaptic surrogates is accompanied by the retraction of GABApre axons from the ventral spinal cord. Thus the recognition of proprioceptive sensory terminals by GABApre axons is absolute rather than hierarchical.

What might explain the remarkable stringency with which GABApre neurons form synaptic connections with sensory terminals? One potential clue comes from the observation that the program of GABApre sensory terminal recognition extends

beyond proprioceptors to include cutaneous sensory neurons. The axons and terminals of sensory neurons are the only neuronal elements in the spinal cord that originate from the peripheral, rather than central nervous system. So, by virtue of their neural crest origin (Marmigere and Ernfors, 2007), the terminals of primary sensory neurons may express recognition cues that are absent from neurons of CNS origin. Our findings show that GABApre neurons are programmed to seek out these sensory-specific labels, to the exclusion of all others. In this view, the formation of synapses between neurons of CNS origin might adhere to the more conventional hierarchical recognition plan, a possibility that needs to be tested. Intriguingly, chemosensory inputs in *C. elegans* and *Drosophila* are subject to presynaptic inhibitory control (Chalasan et al., 2007; Olsen and Wilson, 2008), raising the possibility that stringent programs of sensory synaptic recognition also operate during the construction of invertebrate neural circuits.

The existence of a stringent molecular program devoted to the formation of axo-axonic inhibitory contacts with sensory afferent terminals also helps to explain differing strategies of presynaptic inhibition in mammalian CNS circuits. In most regions of the CNS presynaptic inhibitory control is achieved without the need for direct axo-axonic contact, by virtue of the activation of presynaptic GABA receptors by transmitter that has spilled over from nearby axon terminals (Smith and Jahr, 2002). The association of presynaptic inhibition with an axo-axonic arrangement is a peculiar feature of synaptic organization at the terminals of many classes of primary afferent neurons – in the vestibular, visual, and olfactory sensory systems (Kidd, 1962; Walberg, 1965; Holstein et al., 1999). The stringent GABApre recognition system that underlies proprioceptive sensory gating in the spinal cord may therefore direct the assembly of presynaptic inhibitory circuits in other primary sensory processing centers.

### Sensory Signals Induce the Synaptic Differentiation of GABAergic Interneurons

Proprioceptive sensory terminals appear to provide two distinct sets of GABApre synaptic organizing signals: one set that controls bouton size and synaptic protein concentration, and a second devoted to synaptic accumulation of GAD65 (Figure 7B). The existence of a sensory signal that regulates bouton size and synaptic differentiation can be inferred from the finding that elimination of sensory terminals reduces GAD67, Syt1 and synaptic vesicle marker expression to the low levels normally associated with non-synaptic axonal domains. This signal is evidently not supplied by motor neurons since the GABApre axons that happen to form contacts with motor neurons never acquire bouton-like features and fail to concentrate GABAergic synaptic markers (Figure 7A). The conclusion that GABApre axons require presynaptic inductive signals from sensory terminals contrasts markedly with observations of synapse assembly in certain invertebrate circuits, as well as with studies on cultured vertebrate neurons grown with charged beads, where presynaptic differentiation can proceed in the absence of target cells (Peng et al., 1981; Burry 1982; Prokop et al., 1996; Shen 2004).

A second proprioceptive sensory signaling pathway, mediated by the interaction of BDNF with TrkB receptors, is devoted to the synaptic accumulation of GAD65 in GABApre terminals.

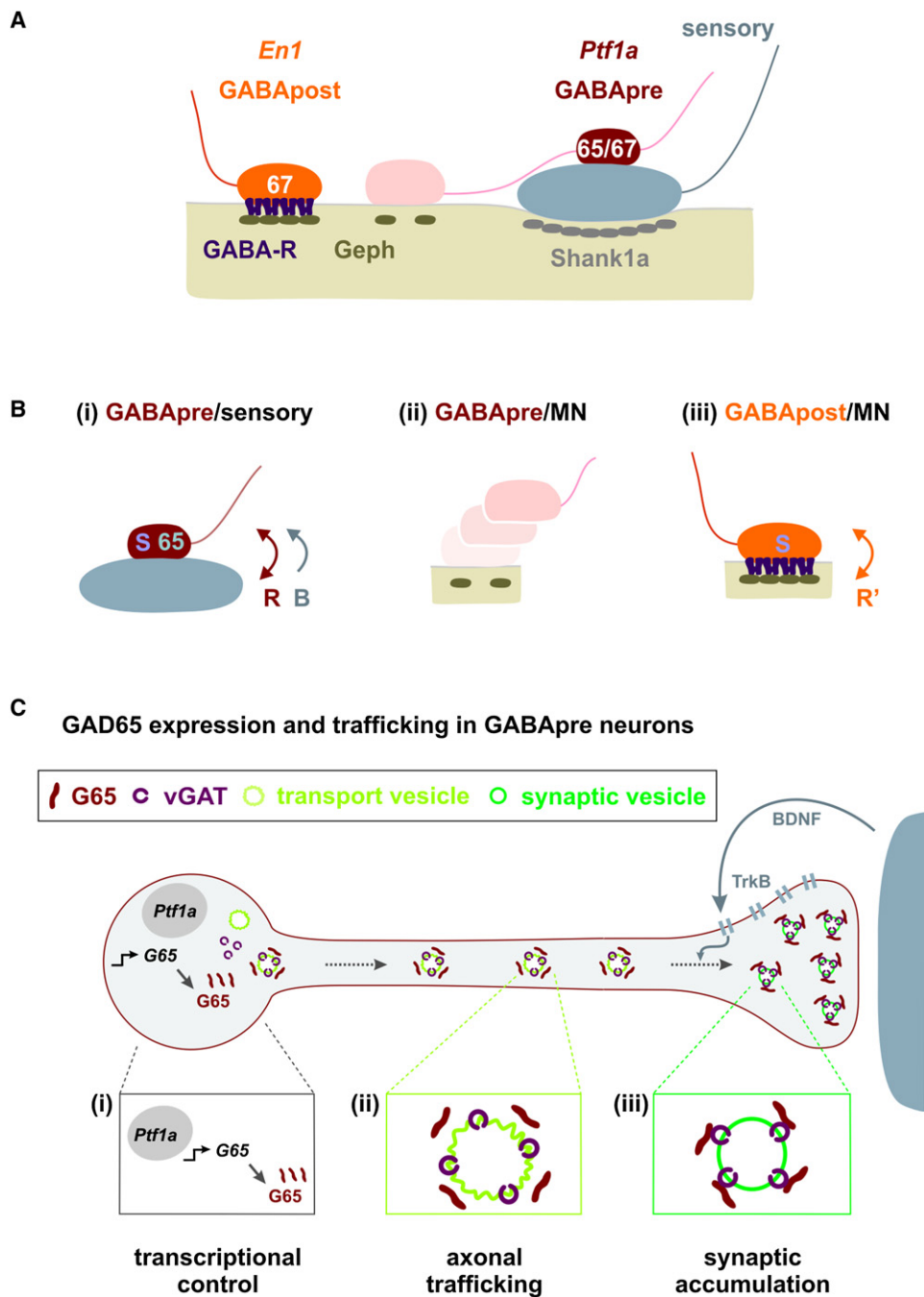


**Figure 7. Sensory Signals Control the Connectivity and Synaptic Differentiation of GABApre Neurons**

(A) Organization of GABApost and GABApre boutons at sensory-motor synapses.

(B) (i) Sensory terminals provide a recognition cue (R) that ensures that GABApre neurons form stable and compact contacts with sensory terminals that express GAD67 (67) and other synaptic proteins (S), and a BDNF-mediated signal (B) that promotes the synaptic accumulation of GAD65 (65). (ii) Motor neurons do not promote stable GABApre contacts or induce synaptic markers in GABApre varicosities. (iii) Motor neurons likely provide a distinct recognition cue (R') that promotes stable GABApost synaptic contacts and induces expression of G67 and other synaptic proteins (S).

(C) The control of synaptic G65 expression in GABApre neurons. (i) An intrinsic *Ptf1a*-dependent transcriptional program determines *Gad65* expression in GABApre neurons. (ii) Trafficking sequences in the N-terminal domain of G65 ensure its transfer to the trans-Golgi network and association with axonal transport vesicles. (iii) Accumulation of G65 in GABApre terminals requires secretion of BDNF from proprioceptive sensory terminals and activation of TrkB signaling in GABApre neurons.

The transport of GAD65 into the axons and terminals of mammalian neurons involves amino-terminal trafficking motifs (Kanaani et al., 2002). Our results reveal a further layer of regulation in GAD65 trafficking, in that the transfer of GAD65 from preterminal axons to synaptic boutons depends on target-derived BDNF signals (Figure 7C). The steps involved in the transfer of GAD65 and other cargoes to mature synaptic vesicles remain obscure (Jin and Garner, 2008), and thus the pathway by which BDNF-TrkB signaling promotes synaptic accumulation of GAD65 is unclear. BDNF-TrkB signaling could regulate the lipid-dependent machinery that directs proteins to synaptic terminals (Kang et al., 2008), promote the stable association of GAD65 with vGAT and other synaptic vesicle proteins (Jin et al., 2003), or the local translation of GAD65.

The emergence of a critical role for proprioceptive sensory terminal signals in the differentiation of GABApre synapses raises the question of whether a parallel retrograde signal is presented by motor neurons to GABApost boutons. Although motor neurons cannot substitute for sensory terminals in the synaptic differentiation of GABApre neurons they do appear to supply an inductive signal that promotes the synaptic differentiation of GABApost boutons. We infer this from the observation that GABApost boutons in contact with motor neurons are significantly smaller than the nearby inflated varicosities of GABApre axons, and by the fact that they concentrate synaptic markers. Sensory terminals and motor neurons may therefore supply distinct retrograde signals that act in dedicated pathways to promote, respectively, the synaptic differentiation of GABApre and GABApost neurons.

Could our findings have relevance for the assembly of GABAergic synapses in other regions of the mammalian CNS? Many classes of GABAergic neurons express GAD65 (Esclapez et al., 1994), and BDNF-TrkB signaling has been widely implicated in the differentiation of GABAergic interneurons (Huang et al., 1999; Rico et al., 2002; Ohba et al., 2005). BDNF may therefore promote synaptic accumulation of GAD65 in other classes of CNS neurons. A program of BDNF-TrkB signaling and GAD65 activity regulates the critical period for ocular dominance plasticity in the mammalian visual cortex (Huang et al., 1999; Hensch, 2005), pointing to one inhibitory circuit in which a dedicated program of synaptic GAD65 accumulation is likely to have functional relevance. The link between BDNF signaling and synaptic GAD65 localization is also intriguing in the context of the activity-dependence of BDNF release from neurons (Hong et al., 2008). Reported instances of activity-dependent regulation of GAD65 expression in other CNS neurons (Hartman et al., 2006) could have their origin in a BDNF-regulated pathway of synaptic GAD65 trafficking. Indeed, we have found that the level of expression of GAD65 in GABApre boutons is markedly reduced in *Egr3* mutant mice (JAK, JNB and TMJ, unpublished observations), a situation in which the activation of proprioceptors is impaired (Chen et al., 2002). Thus, the release of BDNF from proprioceptive terminals may depend on sensory neuron activity.

### Linking Molecular and Functional Programs for Presynaptic Inhibition

Why would GABAergic interneurons involved in presynaptic inhibitory control of sensory-motor transmission take the trouble

to express a distinct set of synaptic proteins? The paucity of GABApre boutons in contact with an individual sensory terminal implies that inhibition of transmitter release requires an unusually effective system for GABA release, in turn demanding a specialized program of GABApre synaptic differentiation.

In many CNS neurons, synaptic expression of GAD65 is needed for efficient GABA release at high stimulation frequencies (Tian et al., 1999)—conditions that result in optimal presynaptic inhibition at sensory-motor synapses (Eccles et al., 1961). Moreover, Syt1 has biochemical properties that permit synchronous transmitter release at central synapses (Maximov and Sudhof, 2005). The specialized molecular features of GABApre inhibitory boutons may therefore fine-tune this set of neurons to the task of presynaptic regulation of sensory input. The compact nature of GABApre boutons may also help to ensure that synaptic vesicles have rapid and unhindered access to presynaptic active zones (Stevens and Williams, 2007), and that individual proprioceptive sensory terminal can be contacted by inhibitory boutons that derive from different GABApre neurons (see Figure S18). This arrangement could provide the flexibility needed for recruitment of different presynaptic inhibitory neurons, according to physiological state (Rudomin, 2009).

## EXPERIMENTAL PROCEDURES

### Mouse Strains

All mouse strains used are described in Supplemental Experimental Procedures.  $\Phi$  indicates a *loxP.STOP.loxP* cassette.

### Histochemistry

In situ hybridization histochemistry was performed on 10–15  $\mu\text{m}$  cryostat sections as described in Supplemental Experimental Procedures.

### Immunohistochemistry

Antibodies are listed in Supplementary Experimental Procedures. Immunohistochemistry was performed on 15–100  $\mu\text{m}$  cryosections and 300  $\mu\text{m}$  vibratome sections as described (Arber et al., 2000; Vrieseling and Arber, 2006) using fluorophore-conjugated secondary antibodies (Jackson Labs). Images were acquired on BioRad MRC 1024 or Zeiss LSM510 Meta confocal microscopes.

### Quantitation of Synaptic Protein Expression

To determine the relative level of protein expression in synaptic terminals, images were obtained on a Zeiss LSM510 Meta confocal microscope, maintaining individual pixel intensities in the linear range for wild-type synapses. We defined the boundary of the synaptic terminal through the use of a soluble GFP marker (wild-type and *Er81* mutant) or the area defined by Syt1 (*BDNF/TrkB* mutants). Average fluorescent pixel intensity/synapse was calculated using histogram function of Adobe Photoshop. For each experimental condition > 100 synapses were analyzed. All values reported are mean  $\pm$  s.e.m. and statistical significance for each comparison was determined using the non-parametric Mann-Whitney U test. Comparisons with  $p < 0.001$  were deemed significant.

### Determination of Synaptic Volume

The volumes of GABApre and GABApost synaptic boutons and GABApre axonal varicosities were determined by calculating the radius of 3-D reconstructed boutons using Zeiss LSM510 software. Calculations and synaptic specificity indices are provided in Supplementary Experimental Procedures.

### Statistical Analysis

For all box plots, the box includes data points between the 25th to 75th percentile of all values, with the line representing the median value. The lines and whiskers represent data between the 9th and 91st percentile and individual dots

represent outlier points. The mean and SEM of values were calculated, and the significance of all pair-wise comparisons was determined using the non-parametric Mann-Whitney U test. Data were considered significant for all *p* values of < 0.01.

## SUPPLEMENTAL DATA

Supplemental Data include Supplemental Experimental Procedures, Supplemental Results and Discussion, Supplemental References, eighteen figures, and one table and can be found with this article online at [http://www.cell.com/supplemental/S0092-8674\(09\)01048-4](http://www.cell.com/supplemental/S0092-8674(09)01048-4).

## ACKNOWLEDGMENTS

We thank A. Liu and S. Doobar for technical assistance; B. Han, M. Mendelsohn, and J. Kirkland for mouse husbandry; S. Morton for antibody generation; J. de Nooij for Dextran fills; A. Todd and R. Hartley for advice; A. Chen and L. Reichardt for BDNF reagents; C. Mason and R. Blazeski for ultrastructural anatomical advice and S. Anderson, S. Arber, R. Axel, J. Bikoff, K. Carniol, C. Henderson, P. Scheiffele, and A. Todd for discussion and comments. J.N.B. was supported by an NIH predoctoral training grant (527975) and a Columbia University Neuroscience Fellowship. J.A.K. was an HHMI Research Associate and supported by a Wellcome Trust Traveling Research Fellowship (IPTRF 064871). T.M.J. is supported by grants from Project ALS, The Wellcome Trust, EU Framework Program 7, and NIH RO1 NS33245. T.M.J. is an HHMI Investigator.

Received: April 22, 2009

Revised: June 12, 2009

Accepted: August 12, 2009

Published: October 1, 2009

## REFERENCES

- Arber, S., Ladle, D.R., Lin, J.H., Frank, E., and Jessell, T.M. (2000). ETS gene *Er81* controls the formation of functional connections between group Ia sensory afferents and motor neurons. *Cell* 101, 485–498.
- Asada, H., Kawamura, Y., Maruyama, K., Kume, H., Ding, R.G., Kanbara, N., Kuzume, H., Sanbo, M., Yagi, T., and Obata, K. (1997). Cleft palate and decreased brain gamma-aminobutyric acid in mice lacking the 67-kDa isoform of glutamic acid decarboxylase. *Proc. Natl. Acad. Sci. USA* 94, 6496–6499.
- Ascoli, G.A., Alonso-Nanclares, L., Anderson, S.A., Barrionuevo, G., Benavides-Piccione, R., Burkhalter, A., Buzsaki, G., Cauli, B., Defelipe, J., Fairen, A., et al. (2008). Petilla terminology: nomenclature of features of GABAergic interneurons of the cerebral cortex. *Nat. Rev. Neurosci.* 9, 557–568.
- Burky, R.W. (1982). Development of apparent presynaptic elements formed in response to polylysine coated surfaces. *Brain Res.* 247, 1–16.
- Cash, S., Chiba, A., and Keshishian, H. (1992). Alternate neuromuscular target selection following the loss of single muscle fibers in *Drosophila*. *J. Neurosci.* 12, 2051–2064.
- Chalasan, S.H., Chronis, N., Tsubozaki, M., Gray, J.M., Ramot, D., Goodman, M.B., and Bargmann, C.I. (2007). Dissecting a circuit for olfactory behaviour in *Caenorhabditis elegans*. *Nature* 450, 63–70.
- Chen, H.H., Tourtellotte, W.G., and Frank, E. (2002). Muscle spindle-derived neurotrophin 3 regulates synaptic connectivity between muscle sensory and motor neurons. *J. Neurosci.* 22, 3512–3519.
- Conradi, S. (1969). Ultrastructure and distribution of neuronal and glial elements on the motoneuron surface in the lumbosacral spinal cord of the adult cat. *Acta Physiol. Scand. Suppl.* 332, 5–48.
- Eccles, J.C., Eccles, R.M., and Magni, F. (1961). Central inhibitory action attributable to presynaptic depolarization produced by muscle afferent volleys. *J. Physiol.* 159, 147–166.
- Esclapez, M., Tillakaratne, N.J., Kaufman, D.L., Tobin, A.J., and Houser, C.R. (1994). Comparative localization of two forms of glutamic acid decarboxylase and their mRNAs in rat brain supports the concept of functional differences between the forms. *J. Neurosci.* 14, 1834–1855.
- Glasgow, S.M., Henke, R.M., Macdonald, R.J., Wright, C.V., and Johnson, J.E. (2005). *Ptf1a* determines GABAergic over glutamatergic neuronal cell fate in the spinal cord dorsal horn. *Development* 132, 5461–5469.
- Glickfeld, L.L., and Scanziani, M. (2006). Distinct timing in the activity of cannabinoid-sensitive and cannabinoid-insensitive basket cells. *Nat. Neurosci.* 9, 807–815.
- Gupta, A., Wang, Y., and Markram, H. (2000). Organizing principles for a diversity of GABAergic interneurons and synapses in the neocortex. *Science* 287, 273–278.
- Hartman, K.N., Pal, S.K., Burrone, J., and Murthy, V.N. (2006). Activity-dependent regulation of inhibitory synaptic transmission in hippocampal neurons. *Nat. Neurosci.* 9, 642–649.
- Hensch, T.K. (2005). Critical period plasticity in local cortical circuits. *Nat. Rev. Neurosci.* 6, 877–888.
- Holstein, G.R., Martinelli, G.P., and Cohen, B. (1999). Ultrastructural features of non-commissural GABAergic neurons in the medial vestibular nucleus of the monkey. *Neuroscience* 93, 183–193.
- Hong, E.J., McCord, A.E., and Greenberg, M.E. (2008). A biological function for the neuronal activity-dependent component of *Bdnf* transcription in the development of cortical inhibition. *Neuron* 60, 610–624.
- Huang, Z.J., Kirkwood, A., Pizzorusso, T., Porciatti, V., Morales, B., Bear, M.F., Maffei, L., and Tonegawa, S. (1999). BDNF regulates the maturation of inhibition and the critical period of plasticity in mouse visual cortex. *Cell* 98, 739–755.
- Huang, Z.J., and Scheiffele, P. (2008). GABA and neuroligin signaling: linking synaptic activity and adhesion in inhibitory synapse development. *Curr. Opin. Neurobiol.* 18, 77–83.
- Hughes, D.I., Mackie, M., Nagy, G.G., Riddell, J.S., Maxwell, D.J., Szabo, G., Erdelyi, F., Veress, G., Szucs, P., Antal, M., et al. (2005). P boutons in lamina IX of the rodent spinal cord express high levels of glutamic acid decarboxylase-65 and originate from cells in deep medial dorsal horn. *Proc. Natl. Acad. Sci. USA* 102, 9038–9043.
- Jankowska, E., and Puczynska, A. (2008). Interneuronal activity in reflex pathways from group II muscle afferents is monitored by dorsal spinocerebellar tract neurons in the cat. *J. Neurosci.* 28, 3615–3622.
- Jin, H., Wu, H., Osterhaus, G., Wei, J., Davis, K., Sha, D., Floor, E., Hsu, C.C., Kopke, R.D., and Wu, J.Y. (2003). Demonstration of functional coupling between gamma-aminobutyric acid (GABA) synthesis and vesicular GABA transport into synaptic vesicles. *Proc. Natl. Acad. Sci. USA* 100, 4293–4298.
- Jin, Y., and Garner, C.C. (2008). Molecular mechanisms of presynaptic differentiation. *Annu. Rev. Cell Dev. Biol.* 24, 237–262.
- Jonas, P., Bischofberger, J., Fricker, D., and Miles, R. (2004). Interneuron Diversity series: Fast in, fast out—temporal and spatial signal processing in hippocampal interneurons. *Trends Neurosci.* 27, 30–40.
- Kanaani, J., el-Husseini Ael, D., Aguilera-Moreno, A., Diacovo, J.M., Bredt, D.S., and Baekkeskov, S. (2002). A combination of three distinct trafficking signals mediates axonal targeting and presynaptic clustering of GAD65. *J. Cell Biol.* 158, 1229–1238.
- Kang, R., Wan, J., Arstikaitis, P., Takahashi, H., Huang, K., Bailey, A.O., Thompson, J.X., Roth, A.F., Drisdell, R.C., Mastro, R., et al. (2008). Neural palmitoyl-proteomics reveals dynamic synaptic palmitoylation. *Nature* 456, 904–909.
- Kidd, M. (1962). Electron microscopy of the inner plexiform layer of the retina in the cat and the pigeon. *J. Anat.* 96, 179–187.
- Kubota, Y., and Kawaguchi, Y. (2000). Dependence of GABAergic synaptic areas on the interneuron type and target size. *J. Neurosci.* 20, 375–386.
- Li, W.C., Cooke, T., Sautois, B., Soffe, S.R., Borisyuk, R., and Roberts, A. (2007). Axon and dendrite geography predict the specificity of synaptic connections in a functioning spinal cord network. *Neural Dev.* 2, 17.

- Marmigere, F., and Erfors, P. (2007). Specification and connectivity of neuronal subtypes in the sensory lineage. *Nat. Rev. Neurosci.* *8*, 114–127.
- Maximov, A., and Sudhof, T.C. (2005). Autonomous function of synaptotagmin 1 in triggering synchronous release independent of asynchronous release. *Neuron* *48*, 547–554.
- Monyer, H., and Markram, H. (2004). Interneuron Diversity series: Molecular and genetic tools to study GABAergic interneuron diversity and function. *Trends Neurosci.* *27*, 90–97.
- Ohba, S., Ikeda, T., Ikegaya, Y., Nishiyama, N., Matsuki, N., and Yamada, M.K. (2005). BDNF locally potentiates GABAergic presynaptic machineries: target-selective circuit inhibition. *Cereb. Cortex* *15*, 291–298.
- Olsen, S.R., and Wilson, R.I. (2008). Lateral presynaptic inhibition mediates gain control in an olfactory circuit. *Nature* *452*, 956–960.
- Peng, H.B., Cheng, P.C., and Luther, P.W. (1981). Formation of ACh receptor clusters induced by positively charged latex beads. *Nature* *292*, 831–834.
- Prokop, A., Landgraf, M., Rushton, E., Broadie, K., and Bate, M. (1996). Presynaptic development at the *Drosophila* neuromuscular junction: assembly and localization of presynaptic active zones. *Neuron* *17*, 617–626.
- Rico, B., Xu, B., and Reichardt, L.F. (2002). TrkB receptor signaling is required for establishment of GABAergic synapses in the cerebellum. *Nat. Neurosci.* *5*, 225–233.
- Rudomin, P. (2009). In search of lost presynaptic inhibition. *Exp. Brain Res.* *196*, 139–151.
- Sanes, D.H., and Poo, M.M. (1989). In vitro analysis of position- and lineage-dependent selectivity in the formation of neuromuscular synapses. *Neuron* *2*, 1237–1244.
- Shen, K. (2004). Molecular mechanisms of target specificity during synapse formation. *Curr. Opin. Neurobiol.* *14*, 83–88.
- Shen, K., Fetter, R.D., and Bargmann, C.I. (2004). Synaptic specificity is generated by the guidepost protein SYG-2 and its receptor, SYG-1. *Cell* *116*, 869–881.
- Shen, K., and Bargmann, C.I. (2003). The immunoglobulin superfamily protein SYG-1 determines the location of specific synapses in *C. elegans*. *Cell* *112*, 619–630.
- Smith, T.C., and Jahr, C.E. (2002). Self-inhibition of olfactory bulb neurons. *Nat. Neurosci.* *5*, 760–766.
- Sotelo, C. (1990). Cerebellar synaptogenesis: what we can learn from mutant mice. *J. Exp. Biol.* *153*, 225–249.
- Stepanyants, A., Tamas, G., and Chklovskii, D.B. (2004). Class-specific features of neuronal wiring. *Neuron* *43*, 251–259.
- Stepien, A.E., and Arber, S. (2008). Probing the locomotor conundrum: descending the 'V' interneuron ladder. *Neuron* *60*, 1–4.
- Stevens, C.F., and Williams, J.H. (2007). Discharge of the readily releasable pool with action potentials at hippocampal synapses. *J. Neurophysiol.* *98*, 3221–3229.
- Thomson, A.M., and Morris, O.T. (2002). Selectivity in the inter-laminar connections made by neocortical neurones. *J. Neurocytol.* *31*, 239–246.
- Tian, N., Petersen, C., Kash, S., Baekkeskov, S., Copenhagen, D., and Nicoll, R. (1999). The role of the synthetic enzyme GAD65 in the control of neuronal gamma-aminobutyric acid release. *Proc. Natl. Acad. Sci. USA* *96*, 12911–12916.
- Vrieseling, E., and Arber, S. (2006). Target-induced transcriptional control of dendritic patterning and connectivity in motor neurons by the ETS gene *Pea3*. *Cell* *127*, 1439–1452.
- Walberg, F. (1965). Axoaxonic contacts in the cuneate nucleus, probable basis for presynaptic depolarization. *Exp. Neurol.* *13*, 218–231.
- Windhorst, U. (1996). On the role of recurrent inhibitory feedback in motor control. *Prog. Neurobiol.* *49*, 517–587.